AAS-22-133

NEO-MAPP μLANDER GN&C FOR SAFE AUTONOMOUS LANDING ON SMALL SOLAR SYSTEM BODIES

Edoardo Caroselli*, Frederik Belien†, Albert Falke‡, Roger Förstner§, and Fabio Curti**

Current missions on Small Solar System Bodies (SSSB) imply long surveying and characterization phases before surface landing is attempted, which decrease time for potential surface activities. The proposed mission concept aims to initiate surface interaction early after arrival in the vicinity of the target SSSB. The lander architecture is designed to allow a safe soft landing and to allocate selected payload developed in the NEO-MAPP study from the European Commission. In addition, a GNC system is developed to run autonomously and enable the spacecraft to safely meet its scientific and mission objectives. Robustness is a major system driver due to the uncharacterized irregular gravity field and limited prior knowledge of the surface as a consequence of the early deployment. Autonomy is fundamental due to long communication delays, and it is addressed via a vision-based solution for navigation and hazard detection and avoidance. In this paper, a μLander mobility backpack is designed as the GNC system to cope with these restrictions within a limited mass budget. The mission reference scenario is based on the DART-Hera environment and operations. Firstly, the system drivers and requirements are identified, and a GNC subsystem design is derived to softly land on the surface. Different avionics suites are compared, traded off, and one is selected. Operational strategies and solutions selection are detailed with strong focus on vision-based technologies to comply with the mass limitation. The developed operational concept and the selected GNC design enable a safe autonomous landing to increase mission lifetime and scientific return of upcoming SSSB missions.

INTRODUCTION

The in situ exploration of Small Solar System Bodies (SSSB), mostly asteroids and comets, is currently at the forefront of planetary sciences. Those bodies provide a window into the past of the Solar System. Asteroids, in particular, are the remnants debris from the planetary formation.

* PhD Candidate, TESOA1, Airbus Defence and Space GmbH, *Claude-Dornier-Str., 88090 Immenstaad, Germany*.
† MSc. GNC/AOCS Development Engineer & Architect, TESOA1, Airbus Defence and Space GmbH.
‡ Programs and Project manager, TSEAZ , Airbus Defence and Space GmbH.
§ Professor, University of the German Armed Forces, Institute of Space Technologies and Space Applications, Munich.
** Professor, Sapienza University of Rome, Scuola di Ingegneria Aerospaziale, Rome

M. Sandnas, D. B. Spencer (eds.), *Proceedings of the 44th Annual American Astronautical Society Guidance, Navigation, and Control Conference, 2022*, Advances in the Astronautical Sciences 179, https://doi.org/10.1007/978-3-031-51928-4_71

Motivation for the exploration of SSSBs is well-grounded and strong and has encouraged large portions of the planetary science community over the last years[1] as shown by Rosetta, Hayabusa and Osiris-Rex missions.

One of the first mission strategies is to perform a flyby of the target body to gather precious information and collect particles around it[2]. The Rendezvous missions allow more time around the asteroid and, as a consequence, a more extensive survey of the unknown environment[3]. The touch-and-go (TAG) approach[4] only temporarily touches the surface and the sample is obtained via a horn-like fast mechanism. The mission concept is less complex compared to a traditional landing, and currently for large spacecraft no landing has been attempted. Landing has been accomplished for smaller spacecraft (CubeSat or microprobes)[5] because they allow to mitigate the risk of losing the mothership without alter the mission returns of surface measurements[6,7].

Usually, before landing, a longer surveying and characterization phase is needed in the order of several months. During this period the target body is analyzed and a surface map is obtained. However, to increase mission lifetime and mission return it would be beneficial for the mission if the spacecraft would land soon after the rendezvous with the asteroid and the payload should rapidly be brought on the surface for direct interaction.[8] To avoid these limitations, the GNC system in this paper is proposed. The proposed architecture is robust to limited a priori knowledge of the environment, and it allows an autonomous, safe and sufficiently precise landing on the asteroid surface for direct measurements. The design is based on a small lander architecture i.e. wet mass is 50 kg with light and off-the-shelf avionics. The GNC algorithms are based on vision-based navigation with hazard detection and avoidance and safe landing site selection.

At first, the mission reference scenario relevant for the GNC design is introduced, then, the GNC system drivers and concept of operations are presented. In addition, the GNC architecture and the selected design are described. Conclusions and future development are finally discussed.

MISSION REFERENCE SCENARIO

The landing scenario describes a mission which puts a spacecraft on the surface of an asteroid for scientific in-situ analysis of the target body. A lander mission is taken into consideration, according to the NEO-MAPP project; all the requirements linked to the cruise and rendezvous phase are neglected in this context.

The surface instrumentation includes bistatic radar, a gravimeter and a seismometer according to the payload developed in NEO-MAPP[9]. The mission scenario is broadly representative of missions with several different types of focus, i.e. surface examinations may serve deflection preparation, scientific interests or resource prospecting purposes.

NEO-MAPP Scenario

The reference scenario for the NEO-MAPP study is the Didymos system environment, as targeted by the DART and Hera missions[10]. Binary targets, i.e. Didymos system, allow to have a more general mission design and to investigate both binary and single bodies maintaining general applicability for versatile scenarios towards different SSSBs. This approach ensures that the developed strategies are applicable to any of the upcoming science and exploration missions without major technology gaps, while of course comparably small adaptions to the specific mission environment cannot be avoided in total.

The Didymos binary system is composed of Didymos and Dimorphos (the primary and secondary body, respectively) with a near Earth orbit around the Sun. The NASA ephemerides are used for the orbit[11]. Dimorphos moves in an approximately circular retrograde orbit with an orbital period of 11.9 hours around Didymos, which equals the rotation period assuming synchronous rotation[12].

The only dynamical parameters measured directly through observations are the orbital period of the secondary around the primary. A shape model of the Didymos primary is based on the past radar observations in combination with light-curve data. Radar data cannot provide a model of the secondary since the signal-to-noise ratio is too weak, echoes are not sufficiently resolved and the rotation coverage is limited[13].

Asteroid Modelling

The two available shape models are enhanced to increase the resolution. To model the system, the available ESA/JPL shape models are used[14]. These models are the most updated knowledge available of the binary system. For the primary body, the Bennu shape model is used[15] and it is rescaled according to Didymos' main moment of inertia (MoI) to simulate the mass properties. Bennu shape model is chosen because it is a high resolution model and the spherical shape fits Didymos estimated shape.

For Dimorphos, the estimated NASA/JPL model consists of a low resolution ellipsoid model which is not sufficient to perform high fidelity landing sequences using vision-based navigation[16].

Figure 1. Synthetic Didymos Environment Generated with ESA/PANGU Software .

Thus, the model is enhanced following three main steps: base model enhancing, surface features addition and albedo matching. The final result is presented in Figure 1. Initially, the high resolution Itokawa asteroid model is rescaled to match Dimorphos' MoI, as done for the primary. This step allows to have increased base surface resolution and to match Dimorphos mass properties. The ESA/PANGU[17] environment simulator is used for the process[18]. Surface features addition consists of adding boulders to the surface according to the rock distribution law provided by Hera reference model[19].

In Figure 2 a comparison is shown between the modelled high-fidelity surface and 67P/Churyumov–Gerasimenko comet surface to check the increased fidelity of this approach for generating synthetic images.

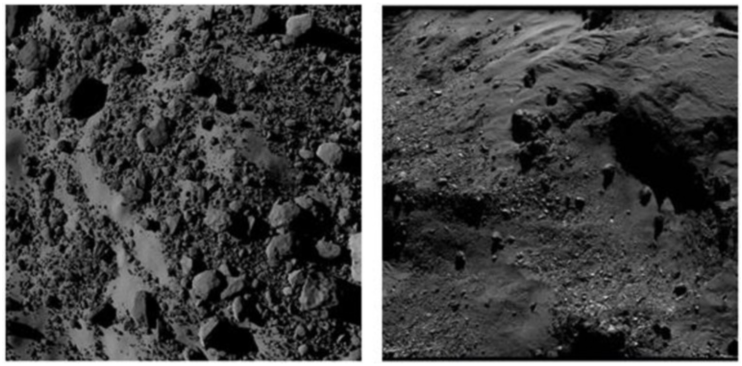

Figure 2. Synthetic Surface Detail (left) and 67P/CG Comet surface (right) .

GNC SYSTEM DRIVERS

The objective of the mission is an autonomous and safe landing of a μLander in a partially known environment from a farther distant orbit i.e. 5 km. In Table 1 the main system drivers are presented and the impact on GNC subsystem is derived.

Table 1. System Driver Identification

System Driver	Impact on GNC	GNC Functionalities
Environment	Limited Knowledge Lack of a-priori landing map	Robust algorithms Physical parameter estimation
Reduced impact of GNC on the SC	Uncoupled avionics from payloads Light and simple architecture	COTS avionics Strongly Mass-optimized GNC
Autonomy	Autonomous decision making No absolute navigation solution	Safe Landing Site detection Surface relative navigation
Safety	Safe Landing Site selection	Safe Landing Site logic Hazard detection and avoidance

Due to the partially known environment the lander shall robustly react to unknown forces both during descent and from contact, the attitude and position shall be always controlled to avoid divergence from the nominal on-board derived guidance profile.

The GNC subsystem shall have a reduced impact on the spacecraft and allow a flexible adaptation to different mission payload architectures. Off-the-shelf components for CubeSat applications are prioritized and selected. Due to these requirements, FDIR represents a significant functionality but it is out-of-the-scope for the present phase.

The long signal flight time in the order of tens of minutes implies that the system shall perform the operations autonomously, i.e. without external intervention from ground or mothership. Autonomy shall be ensured during both nominal decision making process and accidental malfunctions to always prioritize mission survival.

After definition of the target landing site prior to the deployment, the system shall be able to refine the selection according to safety and mission return criteria (e.g. visiting a specific region) during descent, and define on-board an updated landing site.

Finally, the system shall perform a touchdown with minimal translational and rotational velocity. Moreover, it should allow a stable platform for the payload after landing.

CONCEPT OF OPERATIONS

Given the above system drivers the following concept of operations is derived and it is represented in Figure 3. The mission starts with the deployment of the lander from its mothership in the vicinity, i.e. 5 km of the Didymos' system[20]. The lander release point is close enough to safely navigate towards the asteroids and it is far enough away for the safety of the mothership.

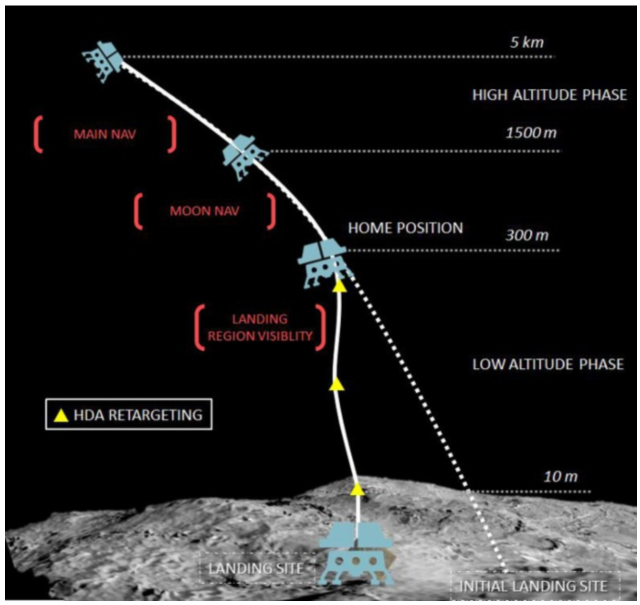

Figure 3. Concept Of Operations Overview.

Landing operations can be partitioned in two operational phases: High Altitude Phase (HAP) and Low Altitude Phase (LAP). The nominal landing site is predetermined at the lander's deployment by ground operators. The HAP operations occur during descent from a distance of 5 km from the target until 300 hundred meters. The aim of this phase is to reach the Home region, which represents the transitioning to the LAP. The Home region is defined with reference to the secondary surface, at a given altitude, i.e. 300 m above the nominal landing site. The LAP is aimed at performing hazard detection and safe landing site selection and navigating to reach the nominal or selected landing site.

Detachment from Mothership

Since the use-case for the mission is the Hera mission, the Hera Payload Deployment Phase (PDP) is assumed as lander initial condition[21]. In particular, Hera will deploy two CubeSats, while in our scenario the µLander will be deployed.

The µLander detachment shall not endanger the Hera orbiter mission by changing the trajectory or attitude constraints. However, Hera is not designed to carry a µLander on the asteroid. As a consequence, the orbital initial condition will be the same as PDP, but the deployment velocity is considered as a free design parameter. The details of the interface between lander and mothership are out of the scope of the work. The trajectory of the lander should allow sufficient time for safe commissioning considering deployment uncertainties, but most of the system is checked out before deployment, except for the actuators.

The landing operation is initiated from Ground. The Ground commanding not only provides the detachment order, but also updates the necessary configuration parameters for the lander and available prior knowledge of the asteroid environment. Depending on the early characterization phase until detachment, more or less a priori information of the asteroid is available.

The initial states of the lander depend both on the knowledge of the mothership's state and on the release mechanism. The mothership's state is estimated via range measurement techniques from the ground, and the inertial attitude is known from the STRs.

The initial condition are defined in accordance with the Hera PDP[22], in Table 2 the initial conditions with related uncertainties are presented.

Table 2. Initial Conditions

State	Nominal value	Uncertainty (3σ)	Comment
Velocity Magnitude [cm/s]	7-14	1	Initial velocity w.r.t. binary system's CoM centered reference frame, assumed inertial during landing.
Velocity Direction [deg]	-90/90	0.5	The angle between Spacecraft-Target line and deployment ΔV. The initial attitude is known very accurately with STRs, and then the uncertainty value is conservative.
Distance [km]	5	0.05	Uncertainty on orbit determination solution

The deployment may be executed either from Early Characterization Phase (ECP) rectangular arc or from Detailed Characterization Phase (DCP1) Z-shaped arc; it is out of the scope of the present study the analysis of deployment operations from Hera spacecraft. As a consequence it can be assumed that the deployment is allowed from any position around the system within the initial conditions boundaries.

Finally, two design criteria for initial conditions are to be considered: firstly, an approach out of the moon orbital plane is preferred because it allows a visual separation between the two bodies for the majority of the landing; in general it reduces the possibility of eclipses. Secondly, an approach from the Sun direction implies optimal illumination condition of the landing site.

Target Landing Site

Several criteria can be identified to select the final condition, i.e. the target landing site. The concept for autonomous operations foresees the possibility to choose a landing region by the operator and then the spacecraft will select the landing site within the region. After the initial decision of the landing region according to scientific interest, two criteria are described to choose the nominal landing region, i.e. angular velocity and eclipse time.

The secondary may be rotating around the Didymos-Dimorphos centre of mass (CoM) axis. In that case, the poles represent the landing sites with minimum angular velocity and as a consequence, the guidance can more easily null the ground relative motion during landing. Moreover, eclipse times are lower at the poles, if the moon is rotating longer illumination condition is possible.

Given the criteria above, optimal landing sites are represented by the poles, in particular the one opposite to Didymos can be reached easier coming from outside the binary system. The outer pole is chosen as a nominal landing site, however the GNC shall allow to land in any site on the secondary surface.

Mission Phases

The mission phases are presented in Table 3. In addition, the switching between phases is done autonomously permitting the mission objectives.

During the Separation and Commissioning Phase, the Lander initiates an avionics system checkout and the navigation status is acquired. During all the operations telemetry is sent back to ground and if the coverage is not available, the data is relayed via the mothership.

Table 3. Mission Phases

Mission Phase	Sub-phase	Functions	GNC Task
Separation & Commissioning	-	Avionics System Check Asteroid Acquisition	Descent towards Home position Pointing Home position
Descent	HAP	Approach the target body Asteroid parameter estimation Telemetry	Environment parameter estimation Descent towards HOME position Pointing Home position
	LAP	Landing site selection Landing preparation Hazard-relative navigation	Descent towards selected landing site Hazard detection and avoidance Pointing selected landing site
Soft Static Landing	Touchdown	Science surface operation	Lander stabilization
	Stabilization		Monitor estimated state

In the Separation and Commissioning Phase, the Lander begins a slow descent for a short period of time, attitude control is granted to begin asteroids acquisition procedures.

The Descent Phase begins autonomously and it is divided into two sub-phases. The High Altitude Phase is from the initial condition to few hundred meters away from Dimorphos with same relative velocity in the end with reference to the target landing site. This phase includes the navigation around both bodies. The switching to the next phase happens as soon as the sensor suite is providing reliable data for the LAP algorithm. As mentioned above, it is also considered to switch at a Home asteroid fixed position; the latter allows easier patching between the two sub-phases and it can be chosen few hundred meters above the target landing site position. The Low Altitude Phase starts from the Home position to the landing site. If no retargeting manoeuvres are occurring the lander has to simply decrease the altitude from the Home position to the surface. Otherwise, landing site selection initiates retargeting for optimal landing site.

Soft Static Landing includes touchdown (and optionally few meters ballistic phase) where the lander keeps a stable attitude and position to allow surface operation.

GNC ARCHITECTURE

Given the aforementioned system drivers and concept of operations, two main architecture elements are traded off: the propulsion system and the availability of a LiDAR sensor. Both these elements have strong implication in the GNC design and functionalities. At the end, an overview of the complete avionics suite is given.

Propulsion System Trade-off

Chemical, cold gas and electric propulsion technologies are considered. Firstly, the $\Delta V = 1\,m/s$ is estimated for the deployment, descent and landing. The estimation is based on the circular restricted three body problem approximation. In particular, it is the energy needed to open the L2 point of the Hill surface with the minimum deployment velocity plus the energy to null the velocity on the surface i.e. soft landing condition. The estimated landing ΔV does not take into consideration real perturbed dynamics, attitude control and potential retargeting maneuvers. The three selected thrusters technology analyzed are presented in Table 4

Table 4. Thrusters Technology

Type	Electric Propulsion	Cold Gas	Chemical Propulsion
Description	ACFT[23]	CGT1 DASA	MR-401 Aerojet
Isp [s]	1500	65	184
Propellant	Xenon	Nitrogen	Hydrazine
Mass [kg] (each)	1.5	0.12	1
Thrust Range [N]	0-0.01	0-0.01	0.07-0.09

Chemical propulsion provides a minimum thrust which is too high compared to cold gas or electrical for the asteroid environment: gravity is extremely weak and sensitive thrusting capabilities are needed. Electrical propulsion may become the preferred solution for many landings or multiple relocations on the surface (e.g. above 100) but for just a single descent is too heavy solution. Cold gas thrusters are selected since they represent a mature technology (TRL 9), they can provide a small impulse bit (60 seconds) and they are a simple and robust technology.

Finally, the cold gas thrusters and fuel low mass makes it possible to avoid using reaction wheel solutions for attitude control by using a thrusters-only architecture.

Camera vs LiDAR Trade-off

Since no absolute measurement is possible, for landing, in-situ information of the surface is required, leading to the selection of either a LiDAR or a camera. Currently, no SSSB mission uses LiDAR on-board of µlanders or CubeSats. Mass and power are the most stringent requirements for the employment of a LiDAR sensor. Also in this case, the current mass allocation given by system design does not allow an existing LiDAR unit on-board. Three different units are traded off[24,25,26] : these options are either too heavy or the operational range is out of our mission scenario i.e. 5 km to surface. It is concluded that a LiDAR-free design is selected. This implies the use of vision-based algorithms for navigation and hazard detection.

Avionics Suite

For the system design, a wet mass of 50 kg has been derived: the allocated mass includes the selected payloads, avionics, fuel and an estimated mass for the additional subsystems, e.g. structure, wiring, etc. The geometrical properties are derived assuming a 35 cm side cube structure. The detailed system design is out of the scope of the present study. However, given the estimated mass budget and geometrical information of the µlander is possible to select the following units.

Table 5. Selected Avionics

Unit	Attitude Navigation	Positional Navigation
Star Tracker	X	-
IMU (Accelerometer + Gyroscope)	X	X
Camera	-	X
Laser Range Finder	-	X
Cold Gas Thrusters	X	X

The attitude is estimated using star trackers and gyroscope measurements provided by the IMU. Taking into consideration the lander size and mass allowance the ST400 from AAC Clyde Space has been selected as a reference sensor for the navigation development[27]. The unit has an accuracy of 120 arcsec and an update rate of 5 Hz. It is radiation tolerant up to 9 krad. The IMU has been selected in collaboration with ISAE/Pioneer project[28], which has the objective of developing an IMU specifically tailored for SSSBs mission. The unit is TRL3 and it is expected to reach TRL 6 by late 2023.

Given the wide difference in altitude between initial condition and touchdown, it is not possible to define an optimal baseline for stereo-vision[29]. In that regards a monocular, i.e. single camera, architecture is derived. The camera field of view (FoV) should allow to correctly frame the two bodies at different mission phases, moreover the resolution drives the HDA capabilities. The IM200 from AAC Clyde Space is selected, the unit is used as a reference but the resolution is modified according to the µlander image processing pipeline. The resolution is 512x512 pixels; the FoV is 30 deg which result in having the primary fill the frame at around 1300 m from the surface and the secondary fill the frame at around 300 m.

The Laser Range Finder is fundamental to have a direct surface range measurement; it is used both for navigation and hazard detection. The baseline unit is DLEM20 from Jenoptik, the unit weighs only 33 g, its range is within the test scenario (up to 5 km) and its accuracy is less than 0.5 m. Finally in Figure 4 the presented units are listed with their navigation applicability.

Figure 4. Sample Unit Selected: IMU, STR, Camera and LRF (from left to right).

GNC DESIGN

One of the key objectives of the NEO-MAPP study is the development of a novel μlander GNC technology. A simulator has been set up for this purpose with the GNC included in an OBC, strictly separated from the simulated world shown in Figure 5. The sensors and actuators form the interface between the OBC and the simulated world. To complete this separation, separate parameters for the assumed prior knowledge are provided. These assumptions on the prior knowledge are drivers for the tuning of the GNC system. The simulator is developed in Matlab/Simulink.

The simulator contains models of the environment (including ephemerides and coordinate transformations), a model of the spacecraft and the dynamics. These models provide inputs to the units, containing the sensors (STR, IMU, Camera and LRF) and actuators (cold gas propulsion). The most complex sensor model is the camera, developed using ESA/PANGU software. The camera and LRF sensor models communicate with the simulator using a TCP/IP connection. The output of the sensors is pre-processed to provide the data in the desired format and frequency to the GNC system. The GNC closes the loop by processing the data and providing commands to the actuators.

Navigation, guidance and control are separated and also the translational and rotational motion are uncoupled, this reduces the complexity and increases the robustness of the subsystem. The sensor models provide the measurement to the navigation block, which uses vision-based navigation both for HAP and LAP. The estimated state is provided to the closed-loop guidance which fuses the information with the autonomous landing site selection block. The hazard detection routine only runs during the LAP at pre-fixed intervals in time. The hazard detection output is used by the guidance for landing site selection. The controller provides the guidance output to the actuator both for translational and attitude control.

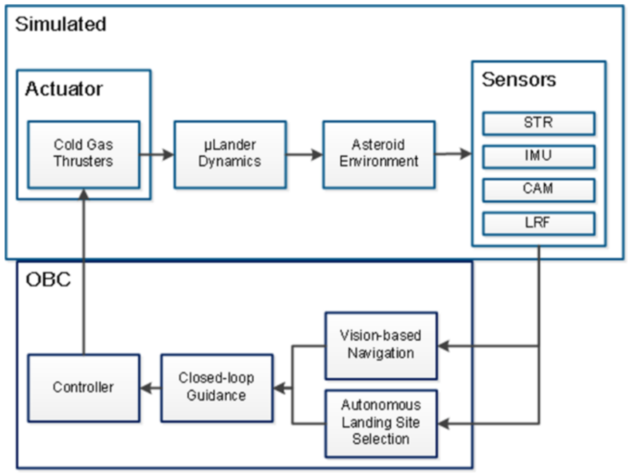

Figure 5. High-level GNC Subsystem Description: Autonomous Landing Site Selection is detailed in Figure 8

Navigation

The navigation uses two different strategies for HAP and LAP: the split between HAP and LAP is driven by the camera and its field-of-view. As shown in Figure 6, the asteroids are both in the field-of-view during HAP and while approaching the primary fill completely the frame. Then, the pointing switch to the secondary, until eventually only a portion of the secondary surface is captured e.g. during LAP. Throughout the complete descent the attitude navigation is done via a standard gyro-stellar estimator using STR and IMU. During HAP a binary centroid-based navigation is implemented[30]. The absolute state, i.e. position and velocity with respect to the system center of mass is estimated using the processed centroid and LRF as measurements. Figure 6 presents a sample HAP navigation processing at two different altitudes.

From 300 m from the surface the secondary completely fills the camera frame and a centroid extraction is no more possible. In fact, during LAP a terrain relative navigation is applied. No prior map of the landing site is used but the relative state with respect to the nominal or selected landing site is estimated. The tracked surface features, the LRF range and the IMU acceleration are the measurement inputs in the navigation filter. In conclusion, it is noted that, given the minimal parallax between different frames during the descent, structure from motion methods or SLAM is not a viable solution[31]; small parallax implies a low observability of 3d information.

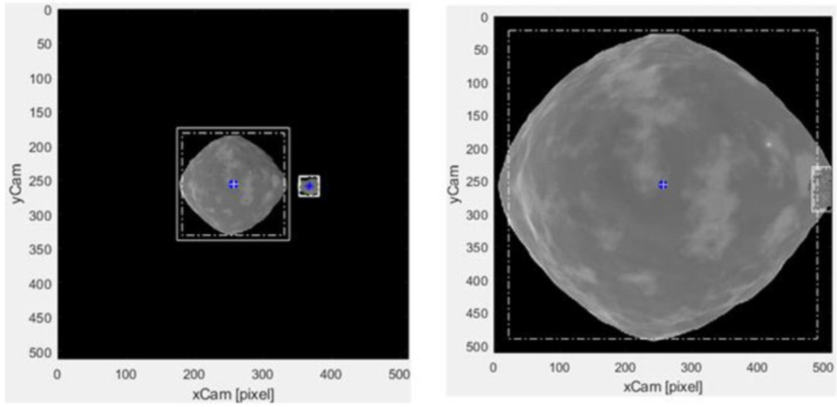

Figure 6. Simulated HAP Navigation Processing: Initial Condition (left) and 1500 m (right).

Guidance

Closed-loop guidance is used during both HAP and LAP, i.e. the current state estimate is used to refine the guidance profile as shown in Figure 7. Given the uncoupled approach between translation and attitude motion, also for guidance, a translational and attitude guidance are identified. Translational guidance is done via constrained terminal velocity guidance which consists in a zero effort miss/ zero effort velocity strategies with constrained terminal velocity[32]. The solution is sub-optimal, but due to the very weak gravitational environment a more computationally expensive optimal solution may be unmotivated, this will be investigated in future works.

Attitude guidance is based on centroid-based pointing; in HAP the camera shall point the primary or secondary body according to their occupancy of the FoV and the switch between the two bodies is done autonomously. In LAP the camera shall point to the target landing site.

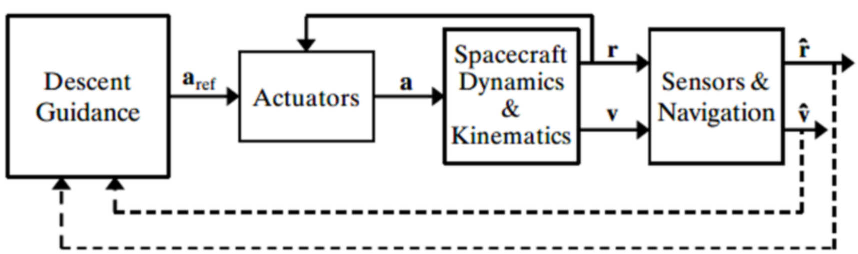

Figure 7. Closed-loop Guidance[33]

Autonomous Landing Site Selection

The Autonomous Landing Site Selection functionality embodies both the hazard detection and landing site selection task. Different hazard criteria are extracted i.e. boulders, shaded areas, slope, roughness and site reachability. The different criteria are processed into maps that are fused together in a Landing Site Logic, when the routine is run a target landing site is provided and if it is safer or better reachable than the current target the new one is selected. The processing pipeline, as shown in Figure 8, utilizes both classical image processing techniques and more advance machine learning based algorithms[18]. The selected landing site is provided to the guidance which computes the trajectory and the attitude to target the site.

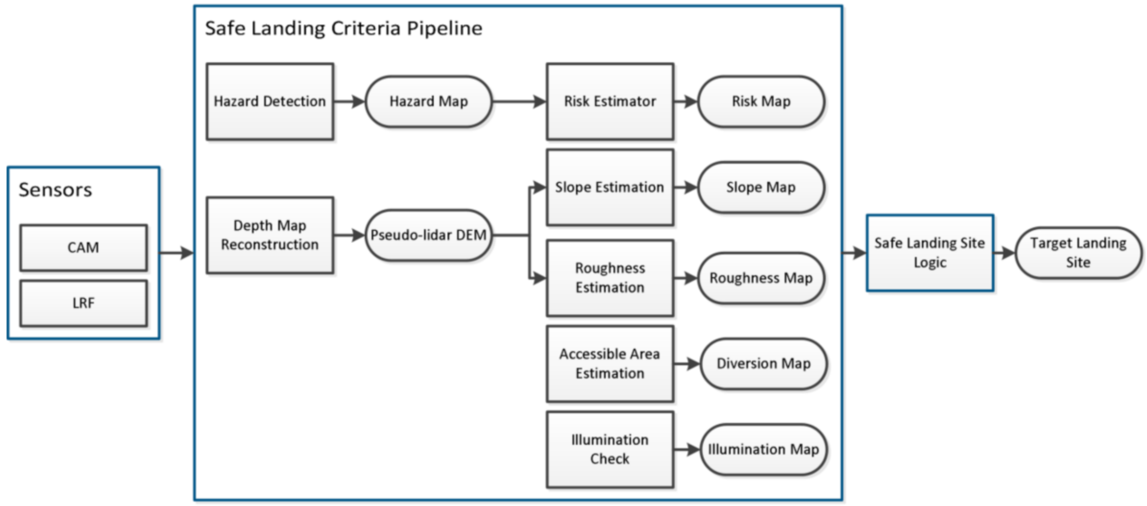

Figure 8. Autonomous Landing Site Selection Processing Pipeline.

Control

The current status of the project assumes an ideal controller, meaning that the control commands are assumed to be able to keep the spacecraft in the desired trajectory. In further stages, standard linear controller and adaptive sliding mode represent potential solution to guarantee a robust approach[34] and they are being investigated. The controllers shall correct any deviations in the trajectory due to unknown or unmodelled dynamics, external disturbances or missing environment parameter. The reference state is compared with the estimated state and the error is minimized by computing the actuators command.

The generated control signal is converted to pulse-width modulated commands for the cold gas thruster model.

CONCLUSION

This paper gives an overview of a µlander technology to enable surface operations for NEO-MAPP scientific payloads. The GNC design has been tailored for the Didymos binary system scenario, representing a challenging mission reference scenario in terms of dynamical complexity (i.e. a binary system), uncertainties (e.g. local gravitation) and selected avionics (i.e. a LiDAR-free design). The concept can be seen as an enabling technology for future SSSB missions. The focus of the work has been on system drivers, requirements and architecture definition. An insight on the trade-offs is presented to describe the decision making. Finally, the main GNC functionalities are presented in the framework of the concept of operations.

The developed GNC is a first step to more autonomous landing operations around SSSBs. Recent missions have relied on detailed characterization of the environment prior to any close-proximity operation. The presented µlander will demonstrate to be less dependent on prior knowledge, due to its sensors and autonomy-enabling GNC algorithms. As a result, minimizing the time between arrival at the target until landing, the mission duration on the surface is increased. The lander autonomy implies increased robustness to the unknown environment and requires less ground support.

FUTURE WORK

This paper has focused on development of μlander technology and its high-level GNC description. Future work will present simulation results and the implementation, verification and validation of the complete GNC loop. Details of the GNC algorithms are[18] or are planned to be published separately. In particular the focus of the upcoming activities will be on LAP navigation and hazard detection and HAP navigation and guidance. A hybrid approach composed of standard and machine learning algorithms will be used.

ACKNOWLEDGMENTS

This project has received funding from the European Union's Horizon 2020 research and innovation programme under grant agreement No 870377.

REFERENCES

[1] Ciesla, F. J., and S. B. Charnley. "The physics and chemistry of nebular evolution." Meteorites and the early solar system II 943 (2006): 209-230.

[2] Perozzi, Ettore, Alessandro Rossi, and Giovanni B. Valsecchi. "Basic targeting strategies for rendezvous and flyby missions to the near-Earth asteroids." Planetary and Space Science 49.1 (2001): 3-22.

[3] Cheng, Andrew F. "Near Earth asteroid rendezvous: mission summary." Asteroids III 1 (2002): 351-366.

[4] Berry, Kevin, et al. "OSIRIS-REx touch-and-go (TAG) mission design and analysis." 36th Annual AAS Guidance and Control Conference. Breckenridge, CO, 2013.

[5] Reill, Josef, et al. "MASCOT—asteroid lander with innovative mobility mechanism." ASTRA 2 (2015): 1-7.

[6] Goldberg, Hannah R., et al. "The Juventas CubeSat in Support of ESA's Hera Mission to the Asteroid Didymos." (2019).

[7] Karatekin, Ozgur, Victor Manuel Moreno Villa, and Hannah Goldberg. "Preliminary investigation of the Juventas CubeSat landing on asteroid Dimorphos." European Planetary Science Congress. 2020.

[8] Pesce, Vincenzo, Ali-akbar Agha-mohammadi, and Michèle Lavagna. "Autonomous navigation & mapping of small bodies." 2018 IEEE Aerospace Conference. IEEE, 2018.

[9] Michel, Patrick, Stephan Ulamec, and Albert Falke. "The European Commission funded NEO-MAPP project in support of the ESA Hera mission: Near-Earth Object Modelling And Payload for Protection." 43rd COSPAR Scientific Assembly. Held 28 January-4 February 43 (2021): 312.

[10] Michel, Patrick, et al. "Science case for the asteroid impact mission (AIM): a component of the asteroid impact & deflection assessment (AIDA) mission." Advances in Space Research 57.12 (2016): 2529-2547.

[11] Bellerose, Julie, Shyamkumar Bhaskaran, and Steven Chesley. "AIDA: Measuring Asteroid Binary System Parameters and DART-Imparted Deflection using the AIM Spacecraft." (2017).

[12] Naidu, S. P., et al. "Radar observations and a physical model of binary near-Earth asteroid 65803 Didymos, target of the DART mission." Icarus 348 (2020): 113777.

[13] Virkki, Anne K., et al. "Near-Earth Object Characterization Using Ground-Based Radar Systems." (2020).

[14] Naidu, S. P., et al. "Radar observations and a physical model of binary near-Earth asteroid 65803 Didymos, target of the DART mission." Icarus 348 (2020): 113777.

[15] Nolan, Michael C., et al. "Shape model and surface properties of the OSIRIS-REx target Asteroid (101955) Bennu from radar and lightcurve observations." Icarus 226.1 (2013): 629-640.

[16] Michel, Patrick, Michael Küppers, and Ian Carnelli. "The Hera mission: European component of the ESA-NASA AIDA mission to a binary asteroid." 42nd COSPAR Scientific Assembly 42 (2018): B1-1.

[17] Parkes, S. M., et al. "Planet surface simulation with pangu." Space ops 2004 conference. 2004.

[18] Caroselli, Edoardo, et al. "Deep Learning-based Passive Hazard Detection for Asteroid Landing in Unexplored Environment" AAS GN&C 2022, Held

[19] Michel, Patrick, et al. "Science case for the asteroid impact mission (AIM): a component of the asteroid impact & deflection assessment (AIDA) mission." Advances in Space Research 57.12 (2016): 2529-2547.

[20] Ferrari, Fabio, et al. "Preliminary mission profile of Hera's Milani CubeSat." Advances in Space Research 67.6 (2021): 2010-2029.

[21] Pellacani, A., et al. "HERA vision based GNC and autonomy." Proceedings of the 8th European Conference for Aeronautics and Space Sciences (EUCASS), Madrid, Spain. 2019.

[22] Goldberg, Hannah R., et al. "The Juventas CubeSat in Support of ESA's Hera Mission to the Asteroid Didymos." (2019).

[23] Vaupel, Max, et al. "The Next Generation milli-Newton µHEMPT as potential main Thruster for small satellites." Proceedings of the 35th International Electric Propulsion Conference (IEPC). 2017.

[24] Gordo, Paulo, et al. "HELENA HERA LIDAR ENGINEERING MODEL ALTIMETER DESIGN." 6th IAA Planetary Defense Conference, 2019.

[25] Mizuno, Takahide, et al. "lIDAR in HAYABUSA Mission." ESCIES. 2nd ESA-NASA Working Meeting on Optoelectronics, Noordwijk, Netherlands, escies. org/download/webDocumentFile. 2006.

[26] Poberezhskiy, Ilya, et al. "Flash lidar performance testing: configuration and results." Laser Radar Technology and Applications XVII. Vol. 8379. International Society for Optics and Photonics, 2012.

[27] Segert, Tom, et al. "Development of the pico star tracker ST-200–design challenges and road ahead." (2011).

[28] Bernauer, Felix, et al. "Exploring planets and asteroids with 6DoF sensors: Utopia and realism." Earth, Planets and Space 72.1 (2020): 1-18.

[29] Woicke, Svenja, and Erwin Mooij. "Stereo vision algorithm for hazard detection during planetary landings." AIAA Guidance, Navigation, and Control Conference. 2014.

[30] Pellacani, A., et al. "HERA vision based GNC and autonomy." Proceedings of the 8th European Conference for Aeronautics and Space Sciences (EUCASS), Madrid, Spain. 2019.

[31] Mur-Artal, Raul, Jose Maria Martinez Montiel, and Juan D. Tardos. "ORB-SLAM: a versatile and accurate monocular SLAM system." IEEE transactions on robotics 31.5 (2015): 1147-1163.

[32] Guo, Yanning, Matt Hawkins, and Bong Wie. "Applications of generalized zero-effort-miss/zero-effort-velocity feedback guidance algorithm." Journal of Guidance, Control, and Dynamics 36.3 (2013): 810-820.

[33] Simplício, Pedro, et al. "Review of guidance techniques for landing on small bodies." Progress in Aerospace Sciences 103 (2018): 69-83.

[34] Lan, Qixun, et al. "Finite-time soft landing on asteroids using nonsingular terminal sliding mode control." Transactions of the Institute of Measurement and Control 36.2 (2014): 216-223.